Stability of Recombinant Yeast Protoporphyrinogen Oxidase: Effects of Diphenyl Ether-Type Herbicides and Diphenyleneiodonium†

Sylvain Arnould,‡ Masayuki Takahashi,§ and Jean-Michel Camadro*,‡

Laboratoire de Biochimie des Porphyrines, Département de Microbiologie, Institut Jacques-Monod, UMR 7592 CNRS−Université Paris 6, Pierre et Marie Curie−Université Paris 7 Denis-Diderot, 2 Place Jussieu, F-75251 Paris Cedex 05, France, and Institut Curie, Bat 110, UMR 216 Institut Curie−CNRS−Université Paris Sud, 15 rue George Clemenceau, 91405 Orsay Cedex, France

Received March 27, 1998; Revised Manuscript Received June 24, 1998

ABSTRACT: Protoporphyrinogen oxidase catalyzes the oxygen-dependent aromatization of protoporphyrinogen IX to protoporphyrin IX and is the molecular target of diphenyl ether-type herbicides. Structural features of yeast protoporphyrinogen oxidase were assessed by circular dichroism studies on the enzyme purified from *E. coli* cells engineered to overproduce the protein. Coexpression of the bacterial gene ArgU that encodes $tRNA_{AGA,AGG}$ and a low induction temperature for protein synthesis were critical for producing protoporphyrinogen oxidase as a native, active, membrane-bound flavoprotein. The secondary structure of the protoporphyrinogen oxidase was 40.0 ± 1.5% α helix, 23.5 ± 2.5% β sheet, 18.0 ± 2.0% β turn, and 18.5 ± 2.5% random-coil. Purified protoporphyrinogen oxidase appeared to be a monomeric protein that was relatively heat-labile (T_m of 44 ± 0.5 °C). Acifluorfen, a potent inhibitor that competes with the tetrapyrrole substrate, and to a lower extent FAD, the cofactor of the enzyme, protected the protein from thermal denaturation, raising the T_m to 50.5 ± 0.5 °C (acifluorfen) and 46.5 ± 0.5 °C (FAD). However, diphenyleneiodonium, a slow tight-binding inhibitor that competes with dioxygen, did not protect the enzyme from heat denaturation. Acifluorfen binding to the protein increased the activation energy for the denaturation from 15 to 80 $kJ \cdot mol^{-1}$. The unfolding of the protein was a two-step process, with an initial fast reversible unfolding of the native protein followed by slow aggregation of the unfolded monomers. Functional analysis indicated that heat denaturation caused a loss of enzyme activity and of the specific binding of radiolabeled inhibitor. Both processes occurred in a biphasic manner, with a transition temperature of 45 °C.

Protoporphyrinogen oxidase (EC 1.3.3.4) is the penultimate enzyme in the heme biosynthetic pathway. It catalyzes the oxidative O_2-dependent aromatization of colorless protoporphyrinogen IX to highly conjugated protoporphyrin IX. Studies on the structure and function of protoporphyrinogen oxidase were stimulated recently by the discovery that diphenyl ether-type herbicides are very potent inhibitors of the protoporphyrinogen oxidase activities of yeast, mammal, and plant mitochondria, and plant chloroplasts in vitro (*1*, *2*). The phytotoxicity of diphenyl ether-type herbicides is light-dependent and involves intracellular peroxidation promoted by the heme and chlorophyll precursor protoporphyrin IX, leading to cell damage and lysis (*3*, *4*).

A better understanding of how diphenyl ether-type herbicides interact with protoporphyrinogen oxidase requires knowledge of the topological features at the active site of the protein. Radiolabeled acifluorfen (*5*) has been used to demonstrate that several chemically unrelated inhibitors of protoporphyrinogen oxidase are all bound to the same site on the plant enzyme (*6*). Specifically bound tritiated acifluorfen is also competitively displaced by protoporphyrinogen IX, the substrate of protoporphyrinogen oxidase (*7*). These results are thus in full agreement with kinetic studies showing that diphenyl ethers are competitive inhibitors (with respect to the tetrapyrrole substrate) of plant, mouse, and yeast protoporphyrinogen oxidase (*8*).

An important component of the enzyme catalytic system is the flavin associated with the enzyme. Yeast and mammalian protoporphyrinogen oxidases are FAD-containing enzymes (*9*−*11*), and sequence analysis of the cloned eukaryotic protoporphyrinogen oxidases shows that all share a common $\beta\alpha\beta$-ADP binding fold characteristic of flavoproteins (*11*−*15*). The role of the flavin in catalysis has been investigated by studying the reactivity of yeast protoporphyrinogen oxidase toward a potential inhibitor of flavoproteins, the diphenyleneiodonium cation (DPI)[1] (*16*). Diphenyleneiodonium and related bis(aryliodonium) compounds appear to be time-dependent, mechanism-based inhibitors of

† This work was supported by grants from the Centre National de la Recherche Scientifique, the Université Paris 7-Denis-Diderot, and the Ministère de l'Education Nationale, de l'Enseignement Supérieur et de la Recherche (Actions Coordonnées Concertées-Sciences du Vivant #5) and the Association de Recherche sur le Cancer (ARC #4005).

* Corresponding author.

‡ Laboratoire de Biochimie des Porphyrines, IJM, Paris.

§ Institut Curie, Orsay.

[1] Abbreviations: 4-nitro-DPI, 4-nitro-2,2′-diphenyleneiodonium; AF, acifluorfen; DZ-AF, diazoketone derivative of AF; CD, circular dichroism; DTT, dithiothreitol; EDTA, ethylenediaminetetraacetic acid; PMSF, phenylmethanesulfonyl fluoride; Tween 80, polyoxyethylene sorbitan monooleate; OG, *n*-octyl β-D-glucopyranoside.

S0006-2960(98)00713-2 CCC: $15.00
Published on Web 08/22/1998

several flavoproteins, such as mitochondrial NADH ubiquinone oxidoreductase (*17*, *18*), neutrophil NADPH oxidase (*19*, *20*), xanthine oxidase (*19*), nitric oxide synthase (*21*), and cytochrome P450 reductase (*22*). DPIs seem to act on the reduced flavins generated during enzyme turnover, that could act as electron donors to the inhibitor, allowing the generation of phenyl radicals that then covalently modify the flavin or some amino acid side chain important in the catalysis (*23*). In addition to inhibiting flavoproteins, alkynyl and aryl mono- and diiodonium salts are potent inhibitors of pyrroloquinoline quinone-related redox processes (*24*, *25*). Diphenyleneiodonium was shown to inhibit yeast protoporphyrinogen oxidase by competing with dioxygen in the reoxidation step of the reduced flavin generated during catalysis that acts as a slow binding inhibitor (*16*), suggesting that there is an isomerization step of the enzyme−inhibitor complexes.

It is necessary to elucidate the topology of the binding sites of the two types of inhibitors of protoporphyrinogen oxidase, diphenyl ethers and diphenyleneiodonium, to obtain a better understanding of the molecular basis of their reactivity. We have therefore determined some of the physicochemical properties of yeast protoporphyrinogen oxidase purified after optimization of the overproduction of the enzyme in *E. coli* cells. The resulting large amounts of purified protoporphyrinogen oxidase were used to study the heat denaturation of the protein, and the effects of inhibitors acting by different mechanisms on the stability and folding of the protein.

EXPERIMENTAL PROCEDURES

Materials. Protoporphyrin IX disodium salt was from Serva; *n*-octyl glucoside was from Alexis Corp.; FAD, urea, and ADP were from Sigma; acifluorfen sodium salt was from ChemService; the tritiated diazoketone derivative of acifluorfen was synthesized by Pr. R. Mornet, Université d'Angers, France (*26*), and 4-nitrodiphenyleneiodonium was synthesized as described by Arnould et al. (*16*). All inhibitors were dissolved in ethanol to give 10 mM stock solutions.

Strains and Plasmid Constructions. The yeast protoporphyrinogen oxidase gene was cloned into pSBETa, a pET3 derivative that carries the ArgU gene (*27*), by PCR amplification of the wild-type *HEM14* gene cloned into the pBS19XS1 plasmid (*12*) using the primers 5′-CCAATGCATATGTTATTACCATTAACAAAGCTAAAACCG-3′ [*Nde*I, (+) strand] and 5′-TCCCCGCGGATCCTTATTTGCTTAGCTGTAAGGCGTC-3′ [*Bam*HI, (−) strand] (initiation and termination codons underlined). The PCR products were purified on agarose gels (JetSorb, Genomed Inc.) and digested with *Nde*I and *Bam*HI. The DNA was repurified (JetSorb, Genomed Inc.) and ligated into the dephosphorylated expression vector pSBETa linearized with *Nde*I and *Bam*HI. The nucleotide sequences of all the constructs were checked by analysis of the plasmid DNA of selected clones.The plasmids were then transformed into the BL21-(DE3) strain of *E. coli*. The T7-RNA polymerase gene was chemically induced by adding 1 mM isopropylthiogalactoside to the cell cultures grown to an OD_{600} of 1−1.5. Induction media were optimized for the synthesis of protoporphyrinogen oxidase. They were Terrific Broth (TB), Luria Broth (LB), or a minimal medium (M63) supplemented with 0.4% glucose, 0.1% casamino acids (Difco), and the antibiotics ampicillin or kanamycin (100 or 70 μg/mL). Induction media were inoculated with cells from fresh cultures grown in LB-Amp/Kan at 37 °C, and 4 generations were grown on the induction medium. The cultures were then chilled on ice for 5 min, isopropylthiogalactoside was added, and the cultures were transferred to microbiological shakers thermostated at the desired temperatures. The cells were collected by centrifugation after various induction times, resuspended in lysis buffer (0.1 M potassium phosphate buffer, pH 7.2, containing 0.1 M KCl, 1% *n*-octyl glucoside, 1 mM EDTA, and 70 μg/mL PMSF), sonicated for 3 × 5 s, and centrifuged. The protoporphyrinogen oxidase activity in the resulting cell-free extracts was measured. The homogenates were diluted 2× in Laemmli sample buffer and processed for electrophoresis as described below.

Purification of Recombinant Yeast Protoporphyrinogen Oxidase. Protoporphyrinogen oxidase was purified from 5 g of cells (wet weight) of the strain BL21(DE3) transformed with the plasmid pSBETa-*HEM14* (clone R8) grown on M63−0.4% glucose medium (*1l*) and induced with 1 mM isopropylthiogalactoside (final concentration) for 15 h at 25 °C. Cells were sonicated in 0.1 M potassium phosphate buffer, pH 7.2, containing 1 mM EDTA and 70 μg/mL PMSF, in ice for 3 × 5 s. The membrane fraction was collected by centrifugation for 1 h at 105000*g*, homogenized (Potter) in the same buffer with 0.1 M KCl, and washed by centrifugation. The pelleted membranes were homogenized (Potter) in 0.1 M potassium phosphate, pH 7.2, containing 1 mM EDTA and 70 μg/mL PMSF and 2% *n*-octyl glucoside and sonicated at 4 °C. The solubilized membrane proteins were extracted by centrifugation for 1 h at 105000*g*. Solid ammonium sulfate (40% saturation, final concentration) was added to the solubilized proteins and the solution stirred for 45 min at 4 °C with a magnetic stirrer. The precipitated proteins were removed by centrifugation for 1 h at 105000*g*. The supernatant containing the soluble protoporphyrinogen oxidase was diluted 2× with 0.1 M potassium phosphate buffer, pH 7.2, and loaded onto a phenyl-Sepharose column (2 × 30 cm) equilibrated with 0.1 M potassium phosphate, pH 7.2, containing 20% glycerol, 1 M KCl, 0.1 mM EDTA, and 70 μg/mL PMSF. The column was washed with 0.01 M potassium phosphate, pH 7.2, 20% glycerol, 0.1 mM EDTA, and 70 μg/mL PMSF. The enzyme was eluted from the column with the same buffer containing 25% sucrose and 1% *n*-octyl glucoside. The active fractions were pooled and concentrated on Amicon YM30 ultrafiltration membranes. The resulting enzyme preparation was apparently homogeneous on SDS−PAGE. The specific activity of the purified protein was 82 000 nmol of protoporphyrinogen oxidized·h^{-1}·mg^{-1}. Oligomerization of purified recombinant yeast protoporphyrinogen oxidase was analyzed by HPLC size-exclusion chromatography using a TSK G3000PW column (0.6 × 30 cm) equilibrated with 0.01 M potassium phosphate, pH 7.2, containing 0.5% *n*-octyl glucoside. The flow rate was 0.6 mL·min^{-1}.

Published procedures were used to prepare extracts of trichloroacetic acid-treated cells (*28*) for SDS−polyacrylamide gel electrophoresis (*29*).

Protoporphyrinogen Oxidase Activity. Protoporphyrinogen oxidase was assayed by measuring the rate of appearance of protoporphyrin fluorescence at 30 °C. The incubation mixture was 0.05 M potassium phosphate buffer, pH 7.2, saturated with air, containing 2 μM protoporphyrinogen IX, 3 mM palmitic acid [in dimethyl sulfoxide (0.5% v/v final concentration)], 5 mM DTT, 1 mM EDTA, and 0.3 mg/mL (final concentration) Tween 80 to ensure maximum fluorescence signal from the protoporphyrin IX, and 0.5% *n*-octyl glucoside. Protoporphyrinogen was prepared by chemical reduction of protoporphyrin IX hydrochloride dissolved in KOH/EtOH (0.04 N/20%) with freshly prepared 3% sodium amalgam (*30*). Protein concentrations were measured by the micro Bradford technique (*31*) on solutions diluted in 0.1 N NaOH. One unit of activity is the amount of enzyme that oxidizes 1 nmol of protoporphyrinogen IX to protoporphyrin IX per hour at 30 °C.

Circular Dichroism. CD measurements were performed with a Jasco J-710 spectropolarimeter using a 0.1 cm path length quartz cuvette. The temperature of the cell was controlled by a programmable Peltier thermoelectric system which allows thermal ramping (melting curve) experiments as well as automated scans at preset temperatures with temperature monitored within the cuvette. All spectra were recorded at 20 °C, and analyzed on accumulation of 10 spectra. The secondary structure of the protein was estimated from the CD spectra using commercial software (Jasco) with the data of Yang (*32*) as references. The software searches for a theoretical spectrum which best fits to experimental data either by considering the estimated protein concentration (finite mode) or by also fitting the protein concentration (infinite mode). The two fitting modes provided very similar results in our study, indicating that the estimation of protein concentration was correct.

Thermal denaturation experiments were done with temperature increases of 1 °C/min. The incubation mixture was 0.05 M potassium phosphate buffer, pH 7.2, containing 0.5% *n*-octyl glucoside. The assays were started at 20 or 30 °C on 10 μM purified enzyme incubated with or without acifluorfen (10−100 μM), 4-nitro-DPI (20−200 μM), FAD (10−50 μM), or ADP (100 μM).

Measurements of the rate of protoporphyrinogen oxidase denaturation were done on samples equilibrated at 20 °C, and the temperature was rapidly raised to higher temperatures. The CD values were measured at 222 nm for 60 min at fixed temperatures. The kinetics of protoporphyrinogen oxidase denaturation were also measured in experiments where the temperature of the sample was increased stepwise, and the CD values were measured at 222 nm for 30 min at each temperature.

The changes in the amplitude of the CD signals obtained during the denaturation of protoporphyrinogen oxidase were analyzed using three models:

(1) Reversible denaturation of the protein followed by slow aggregation of the denatured protein:

$$\text{with } \mathrm{N} \underset{k_2}{\overset{k_1}{\leftrightarrows}} \mathrm{U} \text{ and } 2\mathrm{U} \xrightarrow{k_3} \mathrm{D}$$

$$\text{and } A(t) = A_0 k_1/(k_1 + k_2)[\exp(-(k_1 + k_2)t) + k_2/k_1] \text{ when } k_3 \ll k_2$$

(2) Irreversible denaturation of a mixture of two forms of the protein:

$$\text{with } A_0 = N_1 + N_2 \text{ and } N_1/N_2 = \text{cste};$$

$$\mathrm{N}_1 \xrightarrow{k_1} \mathrm{U} \text{ and } \mathrm{N}_2 \xrightarrow{k_2} \mathrm{U}$$

$$\text{and } A(t) = N_1 \exp(-k_1 t) + N_2 \exp(-k_2 t)$$

(3) Irreversible denaturation of the protein via an intermediate form of the protein with some secondary structure (*33*, *34*):

$$\text{with } \mathrm{N} \xrightarrow{k_1} \mathrm{U} \xrightarrow{k_2} \mathrm{D}$$

$$\text{and } A(t) = [R_1 - R_2(k_1/k_1 - k_2)\exp(-k_1 t)] + R_2(k_1/k_1 - k_2)\exp(-k_2 t)$$

where t is time, A_0 is the amplitude of the signal at time zero, N, U, and D are the native, unfolded, and denaturated (aggregated) states of the enzyme, respectively, and R_1 and R_2 are the contributions to the CD signal of the native (N) and unfolded (U) forms of the protein.

Effects of Temperature on Protoporphyrinogen Oxidase Activity. The initial velocity of protoporphyrinogen oxidase activity was measured on aliquots of enzyme solution, each of which was incubated at an increasing temperature in 5 min steps. The initial temperature was 30 °C, and it was increased to 65 °C by steps with a 5 °C in 10 s rise followed by 5 min at the new temperature, using an Omnibaid 200 PCR thermocycler.

Photolabeling of Binding Sites with Diazo[^{3}H]acifluorfen. Purified protoporphyrinogen oxidase (1 ng) was preincubated with diazo[^{3}H]acifluorfen (25 nM final concentration) in 0.05 M potassium phosphate buffer, pH 7.2, containing 0.5% *n*-octyl glucoside at 30 °C for 5 min in the dark. Nonspecific binding was determined using 15 μM (final concentration) unlabeled acifluorfen as a competitive ligand. The remaining enzyme was treated, in the dark, as for the thermal denaturation of protoporphyrinogen oxidase, but the aliquots were transferred to UV-transparent spectrophotometric plastic cuvettes, placed on a Wilmer Lourmat 302 fluorescence table, and irradiated for 10 min. The lamps emitted broad-spectrum ultraviolet radiation, with a peak emission at 366 nm. The irradiated mixtures were precipitated with 10% trichloroacetic acid (w/v, final concentration) for 30 min at 4 °C, and protein was pelleted by centrifugation at 15 000*g* for 30 min. The proteins were denatured in SDS−PAGE sample buffer and separated by SDS−PAGE. The gels were fixed for 30 min in ethanol/acetic acid/water (30/10/60 per volume), treated with Amplify fluorographic reagent (Amersham) for 30 min, dried under vacuum, and exposed with tritium-sensitive films for 1 week at −80 °C.

RESULTS

Protoporphyrinogen Oxidase Gene Expression. The expression of *HEM14* in pSBETa differed in several major respects from its expression in previously described systems (*12*). The enzyme activity was at least 50 times higher (400 000 units/g of cells fresh weight) than without ArgU (6000 units/g of cells fresh weight), and the protein was produced as a 60 kDa membrane-bound protein. These

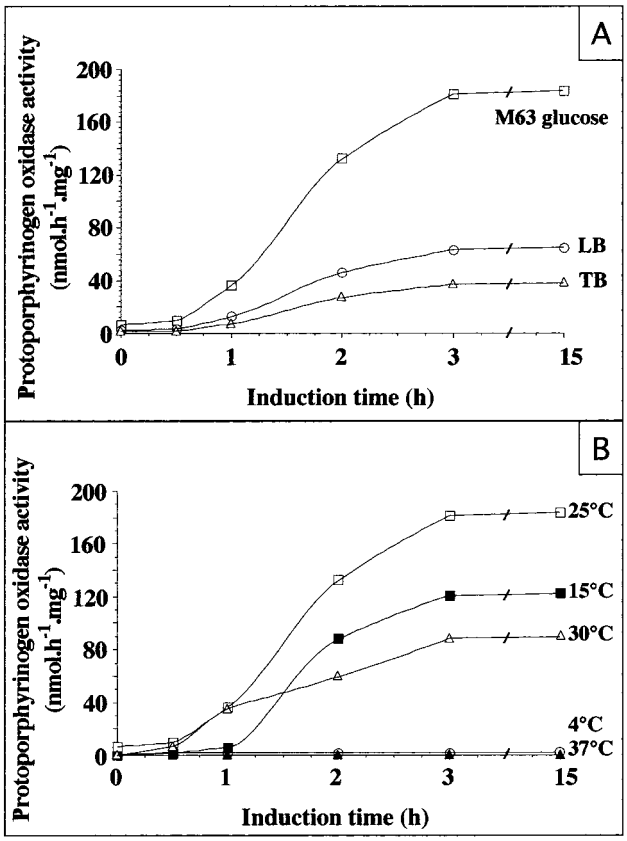

FIGURE 1: Protoporphyrinogen oxidase activity recovery as a function of (A) induction medium (cell grown on LB at 37 °C, induction at 25 °C) and (B) induction temperature (growth at 37 °C and induction in M63−0.4% glucose).

results indicated that the synthesis of yeast protoporphyrinogen oxidase was considerably improved by the production of large amounts of $tRNA_{arg4}$. We optimized the production of the yeast enzyme by investigating the effects of induction medium composition and induction temperature. The induction of protoporphyrinogen oxidase synthesis was greater in minimum medium (M63) than in complete (LB) or rich (TB) media (Figure 1A). Further optimization was therefore conducted in M63 medium. The optimum temperature for induction was 25 °C (Figure 1B). Lower or higher temperatures led to much lower activity, with almost no detectable activity in cells induced at 37 °C. However, analysis of the total proteins in cell extracts by SDS−PAGE clearly showed that greater amounts of protoporphyrinogen oxidase were synthesized at 37 °C (data not shown). At this temperature, and to some extent at 30 °C, protoporphyrinogen oxidase was synthesized as an aggregated inactive protein, possibly in inclusion bodies. Addition to the growth and induction media of 20 μM FAD did not prevent the formation of such aggregates. However, growing and inducing the transformed cells in the presence of 20 μM acifluorfen at 37 °C led to the recovery of 5−10% of the maximum protoporphyrinogen oxidase activity obtained under the optimal production conditions. Subsequent studies were done on protoporphyrinogen oxidase from cells induced at 25 °C in M63 medium for 15 h.

Characterization and Purification of Recombinant Yeast Protoporphyrinogen Oxidase. Induction under optimal conditions gave 5 g of induced cells per liter of culture, in which protoporphyrinogen oxidase accounted for up to 20% of the total protein. A typical purification procedure is summarized in Table 1. The precise quantification of the purification factor at each step was not calculated because both detergent extraction of the protein from the membranes and high-salt treatment increased the enzyme activity 2−3-fold. The specific activity of the purified yeast protoporphyrinogen oxidase was 82 000 nmol of protoporphyrin IX oxidized·h^{-1}·(mg of proteins)$^{-1}$. The N-terminal sequence of the purified protein was identical to that predicted from the gene sequence (MLLPLTKLKPR), as found for the protein purified from yeast mitochondria. The absorption spectrum of the purified protein indicated the presence of the flavinic cofactor. After extensive proteolytic digestion of protoporphyrinogen oxidase with proteinase K, the cofactor was analyzed by reversed-phase chromatography and found to have the chromatographic behavior and the spectral characteristics of FAD. Spectrofluorometric quantification of the flavin indicated a 1:1 flavin to protein stoichiometry. Exogenous FAD did not increase the enzyme activity but rather was slightly inhibitory at flavin to protein molar ratios higher than 1:10. The K_m values for protoporphyrinogen (0.1 μM) for the membrane-bound and the purified enzymes were identical. The inhibitions by diphenyl ether-type herbicides, acifluorfen and acifluorfen-methyl, were of the same order of magnitude as those determined for the enzyme produced in a homologous expression system (*12*) with identical values of IC_{50} for the recombinant membrane-bound and purified enzymes. Both the membrane-bound and purified enzymes were specifically photolabeled with an affinity probe, as was the enzyme from a wild-type yeast strain (data not shown). The inhibition by a new type of mechanism-based inhibitor of protoporphyrinogen oxidase, the diphenyleneiodonium cation, was also identical to that of the yeast mitochondrial membrane-bound enzyme (*16*). The kinetic parameters of these inhibitions are summarized in Table 2.

CD Spectrum of Native Yeast Protoporphyrinogen Oxidase. The CD spectra of native protoporphyrinogen oxidase were recorded and analyzed from 300 to 200 nm (Figure 2,

Table 1: Typical Purification of Yeast Protoporphyrinogen Oxidase Produced in 5 g (Fresh Weight) of *E. coli* BL21(DE3) Expressing the *Hem14* Gene Cloned in pSETa

fraction	total act. (nmol·h^{-1})	yield (%)	protein (mg)	sp act (nmol·h^{-1}·mg^{-1})
total cell extract	2 443 760	100	224	10 910
soluble protein	33 716	1.5	60	562
membrane-bound protein	3 068 480	125	166	18 500
membrane fraction with 2% OG	6 793 990	280	165	41 220
solubilized membrane protein	7 417 140	305	96	77 200
ammonium sulfate precipitation	7 220 190	295	89	81 150
phenyl Sepharose	3 583 080	145	45	80 150
purified enzyme	3 362 720	140	41	82 000

Table 2: Kinetic Constants of Recombinant Protoporphyrinogen Oxidase Inhibition by the Diphenyl Ethers Acifluorfen (AF) and Acifluorfen-methyl (AFM) and Diphenyleniodonium (DPI)[a]

inhibitor type	kinetic constant	membrane-bound recombinant protoporphyrinogen oxidase	purified recombinant protoporphyrinogen oxidase
DPEs	IC_{50} of AF (nM)	7.50 ± 0.40	8.25 ± 0.40
	IC_{50} of AFM (nM)	3.10 ± 0.15	3.90 ± 0.20
DPI	K_i (nM)	50 ± 2.5	88 ± 4.5
	K_i* (nM)	2.9 ± 0.15	2.6 ± 0.15
	$K_m(O_2)$ (μM)	1.7 ± 0.10	2.0 ± 0.10

[a] Diphenyleneiodoniun is a slow-binding-type inhibitor of protoporphyrinogen oxidase, a competititor of molecular oxygen that induces slow isomerization of the enzyme−inhibitor complex:

$$E + I \overset{K_i}{\leftrightarrow} EI \overset{K_i^*}{\leftrightarrow} E^*I$$

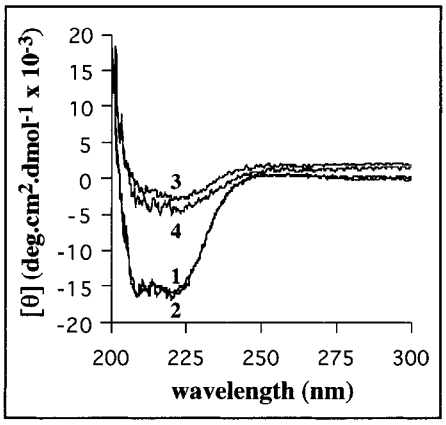

FIGURE 2: CD spectra of purified yeast protoporphyrinogen oxidase (10 μM) with (2, 4) or without (1, 3) 0.1 mM acyfluorfen (AF) recorded at 30 °C (1, 2) and after thermal denaturation at 47 °C (3) or 57 °C (4).

trace 1). The spectra had characteristic features of predominantly α-helical structure with negative minima at 222 and 209 nm. A very intense positive ellipticity in the protein sample below 200 nm prevented effective fitting of the experimental data to theoretical models in the far-UV part of the spectrum. Despite this limitation, the estimated relative amounts of secondary structures in protoporphyrinogen oxidase were 40.0 ± 1.5% α helix, 23.5 ± 2.5% β sheet, 18.0 ± 2.0% β turn, and 18.5 ± 2.5% random-coil, from fitting no less than 10 spectra to the theoretical finite model (*32*). Some positive ellipticity in the 300−250 nm region of the spectrum of heat-denatured protoporphyrinogen oxidase indicated the aggregation of the protein sample. However, the signal/noise ratios were too low to accurately determine the rate of protein aggregation. The competitive inhibitor acifluorfen (AF) did not modify the CD spectrum of native protoporphyrinogen oxidase (Figure 2, trace 2). The spectrum was also unaffected by the other ligands used, 4-nitro-DPI, and/or FAD or ADP.

The unfolding of protoporphyrinogen oxidase undergoing thermal denaturation was monitored by recording the CD signal at 222 nm as a function of temperature (Figure 3A, trace (−)). The first derivative of the melting curve showed a single maximum at 44 ± 0.5 °C (Figure 3B, trace (−)). The melting curve for enzyme incubated in the presence of acifluorfen (1:1 to 1:10 molar ratios) was significantly shifted to higher temperatures (Figure 3A, trace (+)), and the first derivative of the curve showed a single maximum at 50.5 ± 0.5 °C (Figure 3B, trace (+)). The CD spectra recorded at high temperatures (75−80 °C) showed an almost complete

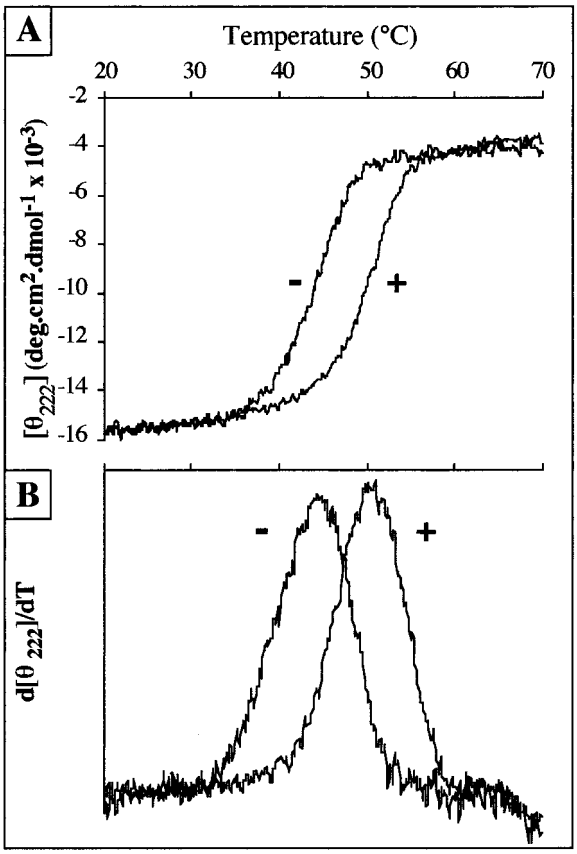

FIGURE 3: (A) Thermal denaturation of yeast protoporphyrinogen oxidase measured by circular dichroism. Purified enzyme (10 μM) was incubated with (+) or without (−) 100 μM acyfluorfen. Temperature increases of 60 °C/h were used, and the CD was measured at 222 nm. (B) First derivative of the melting curves in panel A.

loss of secondary structures in the samples without (Figure 2, trace 3) and with acifluorfen (Figure 2, trace 4), and significant protein aggregation.

The inhibitor 4-nitrodiphenyleneiodonium did not protect the enzyme from thermal denaturation (T_m 44 ± 0.5 °C) (Figure 4), but it significantly potentiated the protective effect of acifluorfen (T_m 52 ± 0.5 °C).

Since yeast protoporphyrinogen oxidase is an FAD-containing enzyme, we studied the influence of FAD and its ADP moiety on the folding of the enzyme. The melting curves showed thermal transitions at 46.5 ± 0.5 °C with FAD alone, which were higher (54 ± 0.5 °C) when the enzyme was incubated with FAD plus acifluorfen. ADP did not

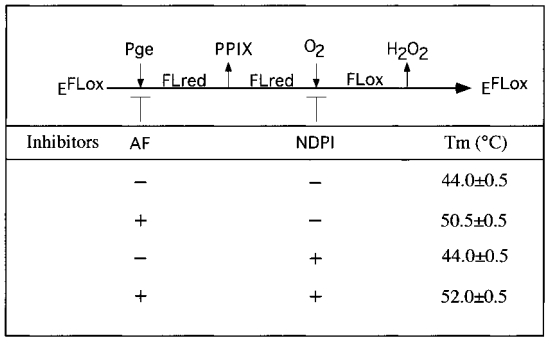

FIGURE 4: Proposed mechanism for yeast protoporphyrinogen oxidase reaction and inhibition by AF and 4-nitro-DPI (NDPI). T_m values are the maxima in the first derivatives of the melting curves of the purified enzyme with (+) or without (−) the inhibitors. E^{FLox}, protoporphyrinogen oxidase with oxidized flavin; E-FLred, protoporphyrinogen oxidase with reduced flavin; Pge, protoporphyrinogen IX; PPIX, protoporphyrin IX.

protect the enzyme from thermal denaturation (T_m 44 ± 0.5 °C).

Kinetics of Yeast Protoporphyrinogen Oxidase Unfolding. Although protoporphyrinogen oxidase was very stable at low temperatures (4−30 °C), with no change in the CD signal at 222 nm over time, it unfolded in a first-order manner when incubated at temperatures where thermal denaturation occurs (Figure 5A, panel (−AF)). In the initial experiments, the protein sample was equilibrated at 30 °C and then rapidly heated with or without acifluorfen (Figure 5A, upper and lower panels). The experimental data were fitted to the equations derived from the three possible unfolding models. The two-step irreversible model did not provide convergent numerical solutions to eq 3 ($R^2 < 0.2$) and was eliminated. The model of irreversible denaturation of a mixture of two independent species provided a good fit of the data to eq 2 ($R^2 > 0.99$) but the N_1/N_2 ratio and the velocity constants calculated varied randomly with the temperature of denaturation. Only the kinetic constants obtained from the model of reversible denaturation of the native monomeric protein followed by slow aggregation of the denatured protein were consistent (Table 3) and allowed us to calculate the activation energy for denaturation: 15 kJ·mol^{-1} without acifluorfen and 80 kJ·mol^{-1} with the inhibitor. Accurate estimation of the kinetic constant of the aggregation of denatured protein was difficult due to the heterogeneity of the aggregates formed. The order of the aggregation reaction is necessarily higher than 2. However, temptative analysis of the experimental data (dN/dt) using the model editor and fitting software Dynafit (*35*) supported the proposed model ($k_3 \ll 2$) despite high relative errors on estimates of k_3. The aggregation step of the heat-denaturation of protoporphyrinogen oxidase needs to be further investigated with different experimental approaches. In the second set of experiments, the protein sample was equilibrated at 20 °C and then rapidly heated to 37 °C with or without acifluorfen and incubated for 30 min at that temperature (Figure 5B, I). The temperature was then raised from 37 to 47 °C to increase the rate of denaturation. In the absence of acifluorfen, the CD signal reached a plateau when the protein was completely unfolded, and there was no further change when the temperature was raised to 57 °C (Figure 5B, I) while in the presence of acifluorfen complete denaturation was obtained at that temperature. The kinetics of denaturation were not modified by preincubating protoporphyrinogen oxidase with both acifluorfen and diphenyleneiodonium (Figure 5B, II). Stoichiometric amounts of the flavin cofactor slowed the unfolding of protoporphyrinogen oxidase in the absence and in the presence of acifluorfen (Figure 5B, III). Because of the spectral interference from the flavin absorption (see noisy signal in Figure 5B, III), we could not perform the experiment with higher flavin concentrations. Further investigation of the FAD effect on protoporphyrinogen oxidase folding was therefore not possible.

Table 3: Kinetic Parameters of the Two Models for Fitting the CD Data at 222 nm at Selected Temperatures (θ)

		model 1[a]		model 2[b]	
AF	θ (°C)	k_1 (min^{-1})	k_2 (min^{-1})	k_1 (min^{-1})	k_2 (min^{-1})
−	37	3.10×10^{-2}	6.25×10^{-3}	1.92×10^{-2}	1.02×10^{-1}
−	44	1.52×10^{-1}	3.83×10^{-2}	2.01×10^{-1}	4.20×10^{-3}
−	47	2.60×10^{-1}	7.38×10^{-2}	3.52×10^{-1}	3.40×10^{-3}
+	47	3.66×10^{-2}	8.96×10^{-3}	9.49×10^{-2}	1.74×10^{-2}
+	50.5	8.35×10^{-2}	2.55×10^{-2}	1.24×10^{-1}	5.32×10^{-3}
+	57	3.46×10^{-1}	8.16×10^{-2}	4.65×10^{-1}	5.64×10^{-3}

[a] Model 1: Reversible denaturation of the protein followed by slow aggregation of the denaturated protein:

with $N \underset{k_2}{\overset{k_1}{\leftrightarrow}} U$ and $2U \rightarrow D$

and $A(t) = A_0 k_1/(k_1 + k_2)[\exp(-(k_1 + k_2)t) + k_2/k_1]$

[b] Model 2: Denaturation of a mixture of two forms of the protein:

with $A_0 = N_1 + N_2$; $N_1 \xrightarrow{k_1} U$ and $N_2 \xrightarrow{k_2} U$

and $A(t) = N_1 \exp(-k_1 t) + N_2 \exp(-k_2 t)$

Functional Analysis of Yeast Protoporphyrinogen Oxidase under Denaturation Conditions. We attempted to correlate the changes in the structure of the protein with its function by measuring protoporphyrinogen oxidase activity remaining in samples of thermally denatured protein. The initial velocity of the enzyme remained almost constant when the enzyme was heated from 4 to 45 °C, but it dropped dramatically at temperatures above 45 °C (Figure 6A).

The capacity of the enzyme to interact specifically with a photoaffinity probe was assessed by analyzing the total and nonspecific labeling of the protein in the denaturation experiments, either by preincubating the enzyme with the labeled ligand or by analyzing the residual binding of the probe to the protein denatured at various temperatures. Preincubation of the enzyme with the diazo[^{3}H]acifluorfen protected protoporphyrinogen oxidase from unfolding as did acifluorfen, and the thermal transition was estimated to occur at 50−55 °C (Figure 6B). The labeling of the protein was mostly specific up to this temperature, but above it, labeling became nonspecific and most of the labeling was detected in aggregated protein that remained on top of the stacking gel in SDS−PAGE. The photoaffinity probe was recovered mostly in such aggregated proteins, when photoaffinity labeling was done after thermal denaturation (Figure 6C). There was more nonspecific labeling under such conditions than previously measured (Figure 6B).

DISCUSSION

This study was designed to examine the structure/function relationships underlying protoporphyrinogen oxidase activity

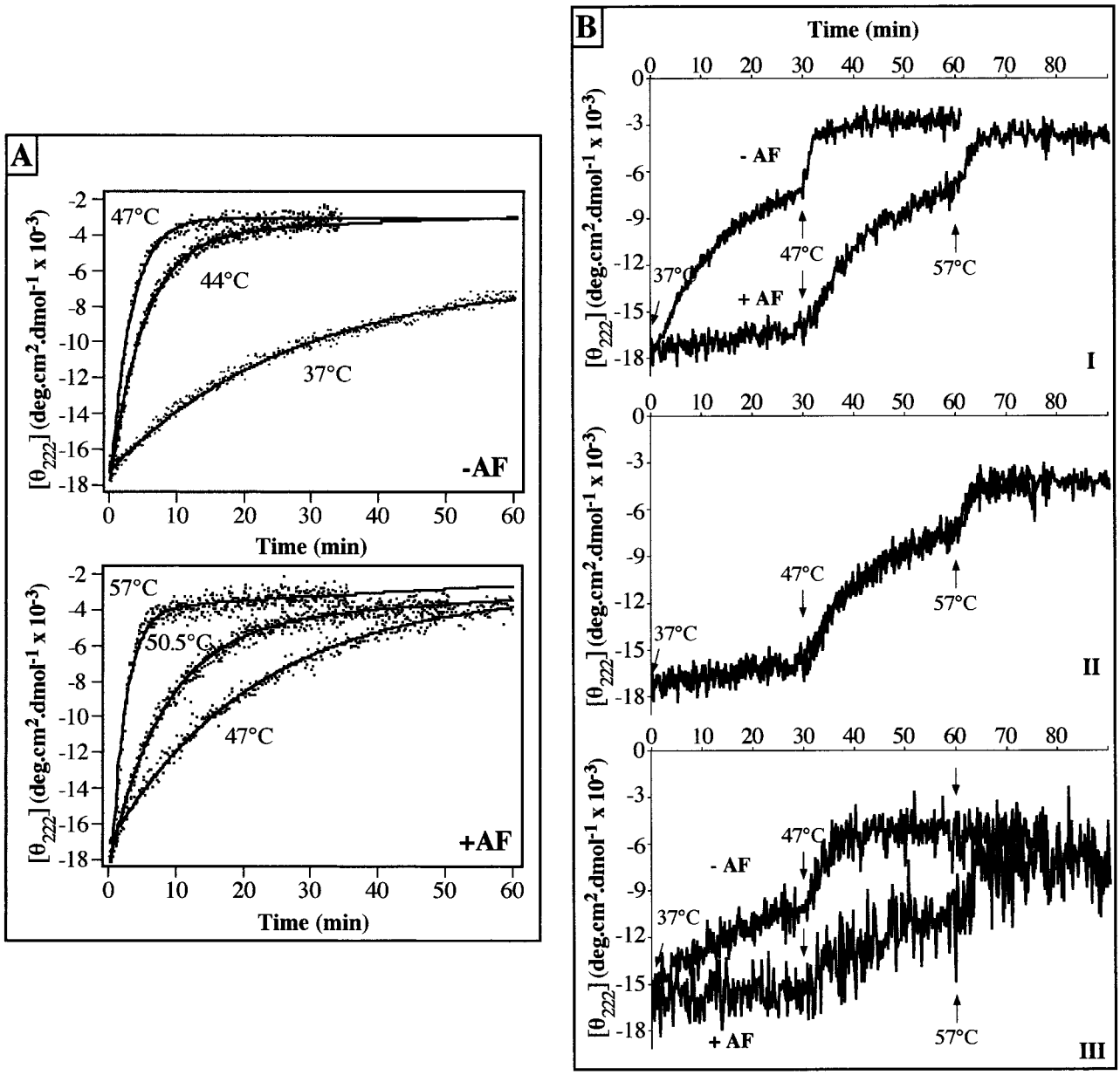

FIGURE 5: (A) Kinetics of thermal denaturation of purified yeast protoporphyrinogen oxidase (10 μM), measured by changes in CD at 222 nm. Measurements were done without (−AF) or with 100 μM acifluorfen (+AF). The initial temperature (30 °C) was immediately raised to the given temperatures, and the variation of CD was measured over 60 min. (B) Kinetics of thermal denaturation of purified yeast protoporphyrinogen oxidase (10 μM), measured by changes in CD at 222 nm. Measurements were done with or without 100 μM acifluorfen (I), with 100 μM acifluorfen with or without 200 μM 4-nitrodiphenyleneiodonium (II), or with 10 μM FAD with or without 100 μM acifluorfen (III). The initial temperature (30 °C) was immediately raised to 37 °C, and the variation of CD was measured over 30 min. The temperature was then raised to 47 °C, and the change in CD was measured for a further 30 min. Last, the temperature was raised to 57 °C, and the change in CD was measured in the final 30 min. Due to high UV absorption by FAD, the signal in 1BIII was noisy.

and its inhibition by diphenyl ether-type herbicides and diphenyleneiodonium. The first step of this work was to develop an efficient system for expressing the yeast gene *HEM14* in *E. coli* that overcomes the problems previously encountered because of the small amounts of protein. Protoporphyrinogen oxidase activity and protein account for less than 0.001% of the membrane-bound protein in commercially available yeast cells or laboratory-grown cells (*9*), and for no more than 0.1% of the membrane-bound protein in yeast cells engineered to overproduce the protein (*12*). Preliminary attempts to use a pT7-5-based system for expressing the yeast protoporphyrinogen oxidase gene in *E. coli* provided a great deal of activity (6000−9000 units/g of cells) (*12*), but the protein is synthesized as, or rapidly processed to, a lower molecular weight polypeptide.

It is now well established that the codon usage in prokaryotic and eukaryotic genes may be very different. It was recently reported that a shortage of the rare $tRNA_{arg4}$ encoded by the ArgU gene in *E. coli* may lead to the incorporation of lysine residues instead of arginine (*36*) and frameshift in the translation of genes, especially when AGA-AGA or AGA-AGG doublets are encountered (*37*). Increasing the availability of the ArgU product significantly improves the expression of recombinant genes in *E. coli* (*27*, *38*, *39*). Since the A+T content of yeast genes is higher than in *E. coli* genes, *S. cerevisiae* genes are more likely to contain frequent Arg_{AGA} codons. Indeed, the 24 arginine codons in the *HEM14* gene include 16 AGA, 6 AGG, and

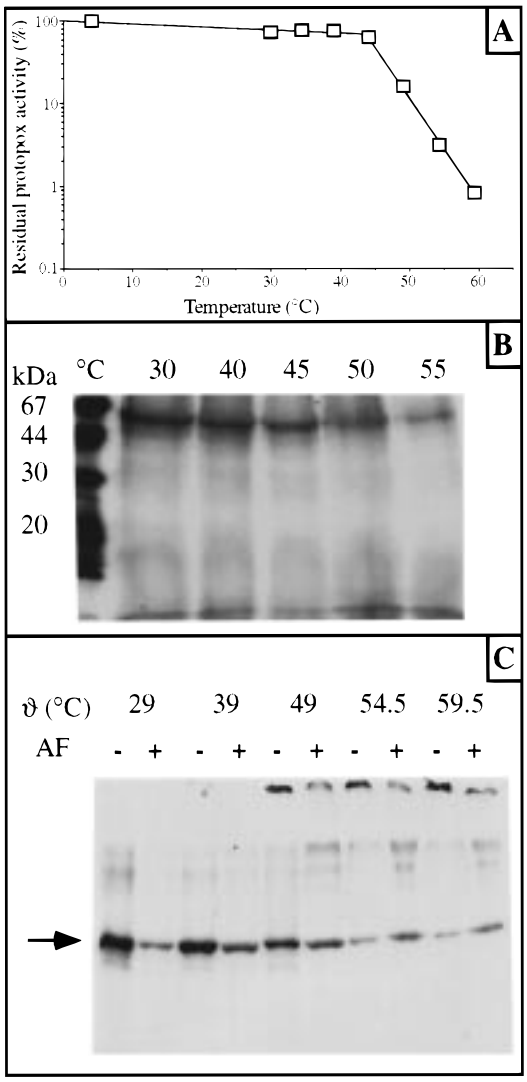

FIGURE 6: Functional analysis of yeast protoporphyrinogen oxidase thermal denaturation. (A) Initial velocity of residual protoporphyrinogen oxidase activity was measured on aliquots of the enzyme solution incubated for 5 min at a series of increasing temperatues. The initial temperature (30 °C) was increased to 65 °C by steps of 5 °C over 10 s followed by 5 min at the new temperature. (B) Photolabeling of binding sites on protoporphyrinogen oxidase with diazo[^{3}H]acifluorfen during the thermal denaturation: the protein (1 ng) was preincubated for 5 min at 30 °C in the dark with diazo-[^{3}H]acifluorfen (25 nM final concentration) and then heated as in panel A above. The solution was irradiated with UV light for 10 min, and precipitated with 10% trichloroacetic acid (w/v, final concentration) for 30 min at 4 °C. The precipitated proteins were denatured in SDS−PAGE sample buffer and separated by SDS−PAGE, fixed for 30 min in ethanol/acetic acid/water (30:10:60 per volume), treated with Amplify fluorographic reagent for 30 min, dried under vacuum, and placed in contact with tritium-sensitive film for 1 week at −80 °C. (C) Photolabeling of binding sites of protoporphyrinogen oxidase with diazo[^{3}H]acifluorfen during thermal denaturation: Purified enzyme (1 ng) was treated for thermal denaturation (see above). Heated samples were incubated with diazo[^{3}H]acifluorfen (25 nM final concentration) for 5 min at 30 °C in the dark without (−) or with (+) an excess of cold acifluorfen (10 μM final concentration), and then irradiated with UV light for 10 min and precipitated with 10% trichloroacetic acid (w/v, final concentration) for 30 min at 4 °C. The precipitated proteins were denatured in SDS−PAGE sample buffer and separated by SDS−PAGE, fixed for 30 min in ethanol/acetic acid/water (30:10:60 per volume), treated with Amplify fluorographic reagent for 30 min, dried under vacuum, and placed in contact with tritium-sensitive films for 1 week at −80 °C.

only 2 CGC codons. This prompted us to investigate the possible involvement of the rare arginine codons in the synthesis of yeast protoporphyrinogen oxidase. Cloning the yeast *HEM14* gene into the pSBETa expression vector that carries the ArgU gene (*27*) considerably improved the synthesis of yeast protoporphyrinogen oxidase in *E. coli*, both quantitatively and qualitatively. The enzyme activity was up to 50 times higher than in the previous system (400 000 units/g of cells), and protoporphyrinogen oxidase accounted for more than 20% of the total protein in cells induced under optimal conditions. The enzyme was then strictly associated with the membrane fraction, where it represented more than 50% of membrane-bound protein. The activity was not washed out of the membranes by high salt. The best induction conditions were a relatively low temperature (25 °C) and a minimum medium (M63-glucose). Although glucose is deleterious for the optimal induction by IPTG of T7 RNA polymerase synthesis cloned under a Lac promotor in the phage DE3, it seems to be essential to slow the cell processes so that native protoporphyrinogen oxidase can be obtained. Low temperature and poor growth medium fulfill this requirement. The availability of $tRNA_{arg4}$ is increased when the growth rate of *E. coli* is decreased (*40*). This, together with the possible synthesis of chaperone proteins under stress conditions for *E. coli*, may be involved in the unusually large amounts of enzyme obtained in a wild-type BL21(DE3) genetic context. As protoporphyrinogen oxidase is strictly associated with the membranes, these amounts compare favorably to those obtained in BL21(DE3) mutants in which large amounts of membrane proteins are synthesized, but mostly as inclusion bodies (*41*).

The association of yeast protoporphyrinogen oxidase with *E. coli* membranes shows that hydrophobicity is an intrinsic property of the protein, with atypical structural determinants that are not identified by classical analysis of the hydropathy plots. However, this association with the membrane fraction may be hampered by aggregation of the protein, as seen in the heterologous expression of protoporphyrinogen oxidases from *B. subtilis*, *M. xanthus*, and the human enzyme (*10*, *13*, *42*). Although the *B. subtilis* enzyme is believed to be bound to peripheral membranes (*43*), it was synthesized in *E. coli* mostly as a soluble enzyme (*42*), as are yeast and mammalian ferrochelatases, the extrinsic mitochondrial membrane-bound enzyme that follows protoporphyrinogen oxidase in the heme biosynthesis pathway (*44*−*46*). Both the *M. xanthus* and the human enzymes are found in the membranes and in the soluble fraction of *E. coli* cells when large amounts are synthesized (*10*, *13*).

The yeast protoporphyrinogen oxidase synthesized in our *E. coli* system is fully active as a 60 kDa polypeptide, as determined both under denaturting (SDS−PAGE) and under native (HPLC−SEC) conditions, indicating that it is a monomeric protein, as is the purified mouse liver protoporphyrinogen oxidase (*47*). Recombinant yeast protoporphyrinogen contained one flavin per monomer. This contrasts with the flavin-to-protein ratios found in the human or *Myxococcus xanthus* enzymes produced in *E. coli* (*10*, *13*) and purified as homodimers with one flavin per dimer. One possible explanation for these discrepancies is that we found the flavin in the yeast enzyme very difficult to extract quantitatively. Complete proteolysis of the polypeptide chain was necessary to extract stoichiometric amounts of the flavin.

The oligomeric status of many membrane-bound proteins may be a function of the concentration of detergent and salts and possibly other factors that may interfere during the experiments. Under our experimental conditions, recombinant protoporphyrinogen oxidase was found to be a monomer, and this allowed us to exclude a first step of dissociation of dimers to monomers in further denaturation studies. The kinetic parameters, K_m for protoporphyrinogen and inhibition by the diphenyl ether-type herbicides acifluorfen and acifluorfen-methyl, of the membrane-bound and purified enzymes are identical to those of the native protein from yeast cells. We investigated the reactivity of the recombinant protoporphyrinogen oxidase toward diphenyleneiodonium cations, a new family of slow-binding inhibitors of protoporphyrinogen oxidase that compete with oxygen in the enzyme reaction and interact with the flavin moiety of the enzyme. The protoporphyrinogen oxidase synthesized in *E. coli* is inhibited by diphenyleneiodonium in a similar way to the yeast membrane-bound enzyme. The kinetic parameters are identical to those previously described (*16*), indicating that the reactivity of the flavin and/or its microenvironment is preserved in the protein synthesized in *E. coli*.

The specific activity of the purified protein is 2-fold higher than that reported for protoporphyrinogen oxidase purified from yeast mitochondrial membranes. It was difficult to measure the total enzyme activity (and therefore its specific activity) during purification because of activation by detergent and high-salt treatment. The hydrophobic interaction chromatography step removed many contaminating proteins (50% by mass), although the apparent specific activity of the enzyme was the same before loading and after elution, due to the parallel loss of both protein and activity. These results suggest that the total activity in the crude extract is underestimated, possibly due to aggregation of the active protein that is solubilized or monomerized by detergent and high salt.

The availability of an efficient heterologous system for producing yeast protoporphyrinogen oxidase overcomes one of the main barriers to investigating the structure of the enzyme and the topology of its active site. It will make possible analysis of the molecular mechanisms involved in the reactivity of wild-type protoporphyrinogen oxidase and variants obtained by site-directed mutagenesis of the yeast protoporphyrinogen oxidase gene, and hence the mechanisms underlying the pathophysiology associated with the enzyme defect (human porphyria) and inhibition (herbicidal effects of DPEs).

Some critical features of the protein can be assessed by measuring the folding and stability of the protein. We used circular dichroism spectroscopy of the protein to address these problems. The CD spectra of native yeast protoporphyrinogen oxidase were recorded from 300 to 195 nm, as there was intense positive ellipticity below 200 nm. The stoichiometric amounts of the flavin cofactor FAD may have caused this interference. However, other flavoproteins such as UDP-*N*-acetylenolpyruvylglucosamine reductase (*48*) or thioredoxin reductase (*49*) have classical far-UV CD spectra, with $\theta_{195}/\theta_{220} \approx 2$, while that of yeast protoporphyrinogen oxidase was $\theta_{195}/\theta_{220} \approx 5$. Similar high $\theta_{195}/\theta_{220}$ ratios are found in β-sheet/coil transitions in model poly(carboxymethylated cysteine) peptides (*50*). Perhaps posttranslational changes in the yeast protoporphyrinogen oxidase cysteine residues may give rise to this CD spectrum. The 350−200 nm spectra of the yeast enzyme had features characteristic of predominantly α-helical structure with negative minima at 222 and 209 nm. The relative proportions of secondary structures in protoporphyrinogen oxidase indicated an α helix content similar to that of the mouse enzyme (*47*). The binding of the diphenyl ether-type inhibitor acifluorfen to yeast protoporphyrinogen oxidase did not modify the general secondary structure of the enzyme. Similarly, the binding of diphenyleneiodonium, which inhibits protoporphyrinogen oxidase by reacting with the flavin cofactor, did not alter the overall folding of the enzyme.

Evaluation of the optimal conditions for expression of yeast protoporphyrinogen oxidase in *E. coli* showed that the induction temperature was critical for producing an active native protein. The overproduced protein was recovered in inactive aggregates after induction above 30 °C. The in vivo-folding of newly synthesized proteins is a complex kinetic process that takes into account the coupling between transcription and translation of mRNA and the influence of many cellular accessory proteins, such as the chaperone proteins [for a review, see (*51*)]. Several factors may affect the proper folding of protoporphyrinogen oxidase, including the correct assembly with the flavin cofactor and the association or integration into the membranes. Slowing the cell processes by using a minimal medium and a low temperature for induction considerably increased the yield of correctly folded protein, but adding acifluorfen to the induction medium considerably improved the production of native protoporphyrinogen oxidase at high temperature, while flavin did not. This suggests that acifluorfen stabilizes the native protein that otherwise may be subjected to heat denaturation in vivo. We therefore studied the folding properties of recombinant protoporphyrinogen oxidase in vitro.

Protoporphyrinogen oxidase appears to be relatively sensitive to thermal denaturation. The T_m (transition temperature at which 50% of the secondary structure is lost) was found to be 44 ± 0.5 °C. The melting curve of the protein had a typical sigmoidal shape, indicating cooperativity in the denaturation process. Acifluorfen protected the protein from thermal denaturation by shifting the T_m to 50.5 ± 0.5 °C, whereas 4-nitro-DPI did not alter the T_m. Equimolar concentrations of acifluorfen and 4-nitro-DPI increased the T_m further to 52 ± 0.5 °C. The inhibition constants of the two compounds are similar (K_i = 1.5 nM for acifluorfen; K_i = 6.4 nM for 4-nitro-DPI), but they act very differently. Acifluorfen competitively inhibits the binding of the substrate to the enzyme, protoporphyrinogen, while 4-nitro-DPI is a competitive inhibitor of oxygen in the reoxidation step of the reduced flavin generated at the active site during catalysis. The thermal denaturation experiments were done on the purified enzyme without its substrate, protoporphyrinogen IX. The flavin cofactor is thus in an oxidized form, so that the isomerization of the enzyme−DPI complex is unlikely. The lack of protection against thermal denaturation by 4-nitro-DPI therefore indicates either that the interaction of 4-nitro-DPI with amino acid residues in the active site of the enzyme involves weak bonds or that the enzyme−DPI complex dissociation constant is high. However, 4-nitro-DPI potentiates the protective effect of acifluorfen (T_m = 55 °C) and may therefore be stabilized into the active site

of the enzyme in the presence of the latter compound. Competition experiments with the two radiolabeled inhibitors are now needed to provide further information on the binding of 4-nitro-DPI to the enzyme in the presence of acifluorfen.

Since protoporphyrinogen oxidase is an FAD-containing enzyme, the proper folding of the native enzyme is likely to involve the correct assembly of the apoprotein with the cofactor. We therefore examined the effects of exogenous FAD and its ADP moiety on the stability of the enzyme. ADP did not alter the T_m of the enzyme, but FAD slightly stabilized it. This modest effect of FAD is not surprising, in view of the complexity of the assembly of the holoprotein in vivo. Studies on the biogenesis of flavoproteins such as human monoamine oxidase B (*52*) or the electron-transfer protein (*53*, *54*) show that, besides the correct folding of the $\beta\alpha\beta$-ADP-binding fold, certain critical acidic residues in the N-terminal end of these proteins and possibly exogenous ADP or AMP are required for the assembly of the holoproteins. ADP plus FAD did not improve the refolding of the denatured protein under our experimental conditions.

The thermal denaturation of yeast protoporphyrinogen oxidase in vitro is a complex process. The main difficulty in establishing a single model for unfolding of the protein is that denatured proteins tend to aggregate. Numerical simulation and experimental data processing suggest that the denaturation of protoporphyrinogen oxidase occurs according to a two-step Lumry−Eyring process (*55*). The first step is an apparently microreversible transition from a native (giving rise to a CD signal) to a denatured (without CD signal) form of the protein. This step obeys pseudo-first-order kinetics. The second step is a second or higher order one, and consists of the slow aggregation of the denatured protein. This leads to an overall irreversible process of denaturation under the experimental conditions used. One factor that promotes the aggregation of the denatured protein is the relatively high concentration of protein used for the CD experiments (0.5−10 μM) which is 2−3 orders of magnitude higher than that required for refolding of the protein (*56*), but it is required for accurate CD spectra. Protoporphyrinogen oxidase is a relatively large protein (539 amino acid residues) and may therefore be a multidomain protein. The sequence analyses of protoporphyrinogen oxidases of various origins all have the N-terminal $\beta\alpha\beta$-ADP-binding fold plus two main domains of homologous sequences linked by a connecting loop (*57*), with the catalytic site presumably associated with the C-terminal domain of the protein. But the characteristic shape of the melting curves of protoporphyrinogen oxidase (with a single T_m) and the kinetic analysis of thermal unfolding suggest that the protein behaves as a single folding domain, and not as the sum of several independent folding structures (see models 2 and 3 under Results). Moreover, acifluorfen does not simply protect the active site; it stabilizes the overall structure of the protein and considerably increases the activation energy required to unfold the protein, from 15 kJ·mol^{-1} for the native protein to 80 kJ·mol^{-1} for the enzyme−inhibitor complex. Although exogenous FAD protects the enzyme against thermal denaturation to some degree, the cofactor is probably essential for stabilizing the protein structure, providing a rigid skeleton for the polypeptide chain. We are currently developing a heterologous expression system to overproduce the protoporphyrinogen oxidase apoprotein in order to examine this problem in more detail.

A critical factor for the protein stability is the interaction of the hydrophobic domains with either lipids (in vivo) or detergent micelles (in vitro, with the purified protein). Raising the temperature during thermal denaturation causes changes in the organization and/or fluidity of the lipid/detergent phases. All the in vitro experiments were done using *n*-octyl glucoside at a final concentration slightly above its critical micellar concentration (0.6 mM). The measured T_m for the protein does not correspond to a phase transition of the detergent and is therefore attributed to changes in the structure of the polypeptide chain. However, the aggregation of the protein at high temperature may well be partly due to the intermolecular interaction of unmasked hydrophobic regions of the protein that are no longer protected at the detergent−protein/micelle interface. A more detailed study of these interactions, together with identification of the substructures in the protein, will become feasible due to recent developments in the methods for differential scanning microcalorimetry.

ACKNOWLEDGMENT

We thank Pr. Pierre Labbe for his interest and valuable advice. The English text was edited by Dr. Owen Parkes.

REFERENCES

1. Matringe, M., Camadro, J. M., Labbe, P., and Scalla, R. (1989) *Biochem. J. 260*, 231−235.
2. Witkowski, D. A., and Halling, B. P. (1989) *Plant Physiol. 90*, 1239−1242.
3. Sandmann, G., Nicolaus, B., and Böger, P. (1990) *Z. Naturforsch. 45C*, 512−517.
4. Scalla, R., and Matringe, M. (1994) *Rev. Weed Sci. 6*, 103−132.
5. Mornet, R., Gouin, L., Matringe, M., Scalla, R., and Swithenbank, C. (1992) *J. Labeled Compd. Radiopharm. 31*, 175−182.
6. Varsano, R., Matringe, M., Magnin, N., Mornet, R., and Scalla, R. (1990) *FEBS Lett. 272*, 106−108.
7. Matringe, M., Mornet, R., and Scalla, R. (1992) *Eur. J. Biochem. 209*, 861−868.
8. Camadro, J. M., Matringe, M., Scalla, R., and Labbe, P. (1991) *Biochem. J. 277*, 17−21.
9. Camadro, J. M., Thome, F., Brouillet, N., and Labbe, P. (1994) *J. Biol. Chem. 269*, 32085−32091.
10. Dailey, T. A., and Dailey, H. A. (1996) *Protein Sci. 5*, 98−105.
11. Dailey, T. A., Dailey, H. A., Meissner, P., and Prasad, A. R. (1995) *Arch. Biochem. Biophys. 324*, 379−384.
12. Camadro, J. M., and Labbe, P. (1996) *J. Biol. Chem. 271*, 9120−9128.
13. Dailey, H. A., and Dailey, T. A. (1996) *J. Biol. Chem. 271*, 8714−8718.
14. Nishimura, K., Taketani, S., and Inokuchi, H. (1995) *J. Biol. Chem. 270*, 8076−8080.
15. Lermontova, I., Kruse, E., Mock, H. P., and Grimm, B. (1997) *Proc. Natl. Acad. Sci. U.S.A. 94*, 8895−8900.
16. Arnould, S., Berthon, J. L., Hubert, C., Dias, M., Cibert, C., Mornet, R., and Camadro, J. M. (1997) *Biochemistry 36*, 10178−10184.
17. Gatley, S. J., and Sherratt, S. A. (1976) *Biochem. J. 158*, 307−315.
18. Ragan, C. I., and Bloxham, D. P. (1977) *Biochem. J. 163*, 605−615.
19. Doussiere, J., and Vignais, P. V. (1992) *Eur. J. Biochem. 208*, 61−71.

20. O'Donnell, V., Tew, D., Jones, O., and England, P. (1993) *Biochem. J. 290*, 41−49.
21. Stuehr, D. J., Fasehun, O. A., Kwon, N. S., Gross, S. S., Gonzalez, J. A., Levi, R., and Nathan, C. F. (1991) *FASEB J. 5*, 98−103.
22. Tew, D. G. (1993) *Biochemistry 32*, 10209−10215.
23. O'Donnell, V. B., Smith, G. C., and Jones, O. T. (1994) *Mol. Pharmacol. 46*, 778−785.
24. Bishop, A., Paz, M. A., Gallop, P. M., and Karnovsky, M. L. (1994) *Free Radical Biol. Med. 17*, 311−320.
25. Gallop, P. M., Paz, M. A., Flückiger, R., Stang, P. J., Zhdankin, V. V., and Tykwinski, R. R. (1993) *J. Am. Chem. Soc. 115*, 11702−11704.
26. O'Connor, N., Mornet, R., Matringe, M., Clair, D., Scalla, R., Fujimoto, T. T., and Swithenbank, C. (1994) *Bioorg. Med. Chem. 2*, 339−342.
27. Schenk, P. M., Baumann, S., Mattes, R., and Steinbiss, H. H. (1995) *BioTechniques 19*, 196−198, 200.
28. Ohashi, A., Gibson, J., Gregor, I., and Schatz, G. (1982) *J. Biol. Chem. 257*, 13042−13047.
29. Laemmli, U. K. (1970) *Nature 227*, 680−685.
30. Poulson, R., and Polglase, W. J. (1975) *J. Biol. Chem. 250*, 1269−1274.
31. Bradford, M. M. (1976) *Anal. Biochem. 72*, 248−254.
32. Yang, J. T., Wu, C. S., and Martinez, H. M. (1986) *Methods Enzymol. 130*, 208−269.
33. Nury, S., Meunier, J. C., and Mouranche, A. (1989) *Eur. J. Biochem. 180*, 161−166.
34. Yoshioka, S., Aso, Y., Izutsu, K.-I., and Kojima, S. (1994) *Pharm. Res. 11*, 1721−1725.
35. Kuzmic, P. (1996) *Anal. Biochem. 237*, 260−273.
36. Calderone, T. L., Stevens, R. D., and Oas, T. G. (1996) *J. Mol. Biol. 262*, 407−412.
37. Spanjaard, R. A., Chen, K., Walker, J. R., and van Duin, J. (1990) *Nucleic Acids Res. 18*, 5031−5036.
38. Ottonello, S., Ballabeni, A., Soncini, C., and Dieci, G. (1994) *Biochem. Biophys. Res. Commun. 203*, 1217−1223.
39. Hua, Z., Wang, H., Chen, D., Chen, Y., and Zhu, D. (1994) *Biochem. Mol. Biol. Int. 32*, 537−543.
40. Dong, H., Nilsson, L., and Kurland, C. G. (1996) *J. Mol. Biol. 260*, 649−663.
41. Miroux, B., and Walker, J. E. (1996) *J. Mol. Biol. 260*, 289−298.
42. Dailey, T. A., Meissner, P., and Dailey, H. A. (1994) *J. Biol. Chem. 269*, 813−815.
43. Hansson, M., and Hederstedt, L. (1994) *J. Bacteriol. 176*, 5962−5970.
44. Gora, M., Grzybowska, E., Rytka, J., and Labbe, B. R. (1996) *J. Biol. Chem. 271*, 11810−11816.
45. Ferreira, G. C. (1994) *J. Biol. Chem. 269*, 4396−4400.
46. Okuda, M., Kohno, H., Furukawa, T., Tokunaga, R., and Taketani, S. (1994) *Biochim. Biophys. Acta 1200*, 123−128.
47. Proulx, K. L., and Dailey, H. A. (1992) *Protein Sci. 1*, 801−809.
48. Axley, M. J., Fairman, R., Yanchunas, J., Jr., Villafranca, J. J., and Robertson, J. G. (1997) *Biochemistry 36*, 812−822.
49. Oblong, J. E., Gasdaska, P. Y., Sherrill, K., and Powis, G. (1993) *Biochemistry 32*, 7271−7277.
50. Maeda, H., Gatto, Y., and Ikeda, S. (1984) *Macromolecules 17*, 2031−2038.
51. Buchner, J. (1996) *FASEB J. 10*, 10−19.
52. Zhou, B. P., Lewis, D. A., Kwan, S.-W., and Abell, C. W. (1995) *J. Biol. Chem. 270*, 23653−23660.
53. Sato, K., Nishina, Y., and Shiga, K. (1992) *J. Biochem. (Tokyo) 112*, 804−810.
54. Sato, K., Nishina, Y., and Shiga, K. (1997) *J. Biochem. (Tokyo) 121*, 477−486.
55. Sanchez-Ruis, J. (1992) *Biophys. J. 61*, 921−935.
56. Jaenicke, R., and Rudolph, R. (1989) In *Protein Structure, a practical approch* (Creighton, T. E., Ed.) pp 191−223, IRL Press, Oxford.
57. Arnould, S., and Camadro, J. M. (1998) *Proc. Natl. Acad. Sci. U.S.A.* (in press).

BI980713I